Biophysical Chemistry 8 (1978) 171–189

ISOLATION AND PHYSICAL STUDIES OF THE INTACT SUPERCOILED, THE OPEN CIRCULAR AND THE LINEAR FORMS OF ColE$_1$-PLASMID DNA

G. VOORDOUW, Z. KAM, N. BOROCHOV and H. EISENBERG
Polymer Department, Weizmann Institute of Science, Rehovot, Israel

Received 12 January 1978

For the study of DNA conformations, conformational transitions, and DNA-protein interactions, covalently closed supercoiled ColE$_1$-plasmid DNA has been purified from cultures of Escherichia coli harboring this plasmid and grown in the presence of chloramphenicol according to the method of D.B. Clewell [J. Bact. 110 (1972) 667]. The open circular and linear forms of the plasmid were prepared by digestion of the covalently closed, supercoiled form with pancreatic deoxyribonuclease and EcoRI-restriction endonuclease, respectively. The linear form was found to be very homogeneous by electron microscopy and sedimenting boundary analysis. Its physical properties ($s^0_{20,w}$ = 16.3 S, $D^0_{20,w}$ = 1.98 × 10^{-8} $cm^2 s^{-1}$ and $[\eta]$ = 2605 ml g^{-1}) have been carefully determined in 0.2 M NaCl, 0.002 M $NaPO_4$ pH 7.0, 0.002 M EDTA, at 23°C. Combination of $s^0_{20,w}$ and $D^0_{20,w}$ (obtained by quasielastic laser light scattering) gave $M_{S,D}$ = 4.39 × 10^6. This value is in reasonable agreement with the molecular weight from total intensity laser light scattering M = 4.30 × 10^6. The covalently closed and open circular forms of the ColE$_1$-plasmid are less homogeneous due to slight cross-contamination and the presence of small amounts of dimers in these preparations. The weight fractions of the various components as determined by boundary analysis or electron microscopy are given together with the average quantities obtained in the same solvent for the supercoiled form ($\langle s^0_{20,w}\rangle_w$ = 25.4 S, $\langle D^0_{20,w}\rangle_z$ = 2.89 × 10^{-8} $cm^2 s^{-1}$, $[\eta]$ = 788 ml g^{-1}, $M_{S,D}$ = 4.69 × 10^6 and M_w = 4.59 × 10^6) and the open circular form ($\langle s^0_{20,w}\rangle_w$ = 20.1 S, $\langle D^0_{20,w}\rangle_z$ = 2.45 × 10^{-8} $cm^2 s^{-1}$, $[\eta]$ = 1421 ml g^{-1}, $M_{S,D}$ = 4.37 × 10^6 and M_w = 4.15 × 10^6). Midpoint analysis of the sedimenting boundaries allows unambiguous determination of the sedimentation coefficients of these two forms: $s^0_{20,w}$ = 24.5 S and $s^0_{20,w}$ = 18.8 S, respectively. Also deduced from total intensity light scattering were radii of gyration R_g (103.5, 134.2 and 186 nm) and second virial coefficients A_2 (0.7, 4.8 and 5.4 × 10^{-4} mole ml/g^2) for the supercoiled, the open circular and linear forms, respectively. The data presented are discussed in relation to the conformational parameters for the three forms in solution.

1. Introduction

A topic of research of considerable current interest is the study of the chromosome, the structural unit of the genome. The physical structure of the eukaryotic chromosome, incorporating the all-important feature of gene expression, is based on well-defined complexes of nucleic acids (mostly DNA) and proteins (a major component of which are the highly basic histones). It is possible, by controlled treatment of eukaryotic nuclei, to reduce the chromosome in size, to remove certain labile components, and to isolate a still biologically active substance, called chromatin [1,2]. Chromatin is a complex of DNA and histones, and has been shown to consist of well-defined repeating units [3] called ν-bodies [4] or nucleosomes [5]. Another approach to the problems of defining chromosome structure was the demonstrated possibility of reconstituting ν-bodies or nucleosomes, and therefore materials to many extents and purposes similar to chromatin, by the controlled interaction of purified DNA and a mixture of histones [6]. Our present work is concerned with the isolation and investigation of conformations and conformational transitions in well-defined DNA samples, in quantities sufficient for detailed physical studies, as well as a detailed study of the complexation with histone and, hopefully, non-histone proteins. The initial study presented here contains part of this investigation, to be pursued further. A preliminary report on the properties of well defined complexes of ColE$_1$-

plasmid DNA and the calf-thymus histones H2A, H2B, H3 and H4 has been presented [7]. Complexes, saturated with histone, were shown to contain histones in excess of the amount usually believed to be associated with DNA in chromatin. We thereupon studied the binding of additional histones to chromatin core particles from calf-thymus [8]. A detailed study of the properties of the saturated plasmid DNA-histone complexes is in preparation [9].

The conformation of double-stranded deoxyribonucleic acid in solution has been subject to active investigation ever since the central role of this molecule was realized [10]. Many DNA's exist in living cells as covalently closed duplexes [11], often with tertiary turns (supercoils). Enzymes exist which are capable of making single-strand breaks with release of the tertiary turns and formation of an open circular conformation or double strand breaks with linearization of the molecules. The mass of chromosomal DNA is gigantic, being of the order of 10^9 daltons in bacteria and in excess of 10^{10} daltons in eukaryotes [12]. Since it is rather difficult to isolate such giant molecules intact, most physical chemical studies in the past have been performed on linear fragments derived from the chromosome. These fragments are much smaller in size and are usually polydisperse. As an example, preparations of double-stranded calf-thymus DNA, which have often been used for study have molecular weights M of about 2×10^7 with a rather broad molecular weight distribution. The problems in studying the conformational properties of such DNA-preparations in solution are well known [13,14] and stem from both the polydispersity and the very size of the molecules in the sample. Fortunately, the molecular weight can be lowered by shearing or sonication, without loss of the double helical character of the DNA, and studied by various means [15], while the polydispersity can be reduced by fractionation methods. Following this procedure Godfrey [16] and Jolly and Eisenberg [17] were able to resolve sonicated calf-thymus DNA into a number of narrowly disperse fractions ($\bar{M}_w/\bar{M}_n \approx 1.04$ to 1.14) with weight-average molecular weights $\bar{M}_w$ ranging from about 0.3 to 3.8×10^6 ($\bar{M}_n$ is the number-average value of M). Determination of molecular weights by sedimentation equilibrium and light scattering, which gave in addition the root-mean-square radius of gyration, permitted calculations of the persistence length a for each fraction [17,18]. The persistence length is a measure of chain flexibility of the Kratky–Porod [19,20] worm-like coil, which is thought to be a most realistic model for the solution conformation of linear DNA [13,14]. Godfrey and Eisenberg [18] deduce that this quantity is invariant over the molecular weight range examined and obtain an average value $a = (60 \pm 6)$ nm. Theoretical curves relating sedimentation coefficients and intrinsic viscosities to molecular weights, calculated with a similar invariant persistence length, closely represented data from several investigators for well characterized DNA samples of various origin, over a molecular weight range from 4×10^4 to 10^8.

An attractive alternative to the widely used method of fractionating polydisperse, sonicated DNA into narrowly disperse fractions is obviously to isolate small molecular weight monodisperse DNA. Such DNA-molecules, like the viral DNA's and the extra-chromosomal bacterial plasmids for instance, are quite common, with molecular weights in the range 10^6–10^8. Apart from the unique size of these molecules, they offer the additional advantage that their supercoiled and open-circular conformations may be isolated intact as well. This is of importance as a proper, complete determination of solution conformation parameters is lacking at present for these two conformations. Bauer and Vinograd [11], in a recent review on circular DNA, report that no experimental evidence was available to indicate what may be the best model for the structure of closed duplex DNA in solution. Unfortunately, many of these small, monodisperse DNA-molecules can be investigated only with difficulty by physical means because relatively large amounts of material (in the milligram range) are required for a complete study. We choose the $ColE_1$-plasmid as the object for our investigations, mainly because the above mentioned limitation can be overcome in this case. Amounts of plasmid DNA comparable to those of the chromosomal DNA can be isolated from E. coli harboring it due to the fortunate circumstance that the plasmid continues to replicate in the presence of chloramphenicol while replication of the chromosomal DNA ceases under these conditions. The plasmid DNA may reach levels as high as 3000 copies per cell [21]. Under these conditions it is free of covalently attached protein [22–26] and is quite homogeneous with respect to molecular weight except for the presence of a small dimer fraction [21]. The $ColE_1$-plasmid has a single cleavage site only for

the restriction enzyme EcoRI [27], allowing linearization of the naturally occurring circular molecule without change in molecular weight. This molecular weight ($\sim 4.2 \times 10^6$, as deduced by electron microscopy) is in a convenient range for light scattering and hydrodynamic studies and the chance of a double-strand breaks in the course of normal handling of solutions is minimal.

The best characterized monodisperse DNA's to date by solution methods are those of several bacterial phages, such as T7 ($\sim 25 \times 10^6$ daltons), T5 ($\sim 70 \times 10^6$ daltons) and T4 ($\sim 112 \times 10^6$ daltons) [28]. Their high molecular weight makes them difficult to handle and solutions of these linear phage DNA's are strongly nonideal even at minute concentrations [29]. It thus appears that extensive physical properties of linear monodisperse DNA are available in a narrow molecular weight range only, and those for covalently closed supercoiled and open circular monodisperse DNA's have been studied even more rarely [30,31].

In the present paper we undertake electron microscopy, sedimentation velocity, viscosity, total intensity and quasi-elastic light-scattering studies, and derive extensive data on all three conformational forms of $ColE_1$-plasmid DNA prior to a study of DNA-histone interactions.

2. Materials and methods

2.1. Materials

Chloramphenicol and ethidium bromide were obtained from Sigma. Yeast extract and casamino acids were from Difco. CsCl (AnalaR) was obtained from BDH. Lysozyme was from Sigma and pancreatic deoxyribonuclease-I* (3100 units/mg) was obtained from Worthington. EcoRI (6000 units/ml in 0.2 M NaCl, 0.005 M KPO_4 pH 7.0, 1.0×10^{-4} M EDTA, 0.0025 M 2-mercaptoethanol, 0.1% Triton X-100 and 50% glycerol) was purchased from Biolabs. Double distilled sterilized water was used throughout. Glassware was sterilized before use. All other chemicals used were reagent grade.

* $ColE_1$-I, $ColE_1$-II and $ColE_1$-III – the covalently closed circular, the open circular and the linear forms of the $ColE_1$-plasmid, respectively; TES – 0.05 M NaCl, 0.005 M EDTA, 0.03 M Tris ph 8.0; DNA'se-I – pancreatic deoxyribonuclease-I; EDTA – ethylenediaminetetraacetic acid; Tris – Tris(hydroxymethyl)aminomethane.

2.2. Preparation of $ColE_1$-I

E.coli (W3110), harboring the plasmid $ColE_1$, was grown at 37°C in shakeflask culture, in 4 ℓ erlenmeyers containing 1 ℓ of M9 medium [21,32], supplemented by 0.5% yeast extract and 0.5% casamino acids. Growth was followed by measuring turbidity in a Klett–Summerson colorimeter by use of a red filter. Solid chloramphenicol (150 mg) was added at a Klett reading of approximately 160 and the flask was left shaking for another 12 h [21]. Cessation of growth was apparent from the constant Klett readings under these conditions. The cells were then harvested by centrifugation (20' at 8000 g, at 4°C). Cells from one liter of culture medium were lysed [21,33] by suspending the cell-pellet in 5 ml of cold 25% sucrose in TES*. Lysozyme (1.0 ml, 5 mg/ml in 0.25 M Tris, pH 8.0) was then added, followed after five minutes by addition of 2.0 ml of EDTA (0.25 M, pH 8.0). The suspension was kept for another five minutes at 0°C under occasional swirling after which the cells were lysed by addition of 8 ml SDS (2% w/v in TES). The extremely viscous suspension was mixed very gently for five minutes after which 5 M NaCl in TES was added to a final concentration of 1 M NaCl. The suspension was stored in the refrigerator (2°C) overnight and was then centrifuged for 1.5 h at 4°C and 37 500 g. This lysis procedure removes essentially all of the chromosomal DNA with most of the plasmid DNA remaining in the supernatant. The latter was dialyzed for 24 h against TES; CsCl was added to $n_D^{24} \approx 1.393$ ($\rho^{24} \approx 1.63$ g/cm^3) and 12.3 ml of this solution was placed in a 5/8 × 3 inch cellulose nitrate tube (Beckman) together with 0.2 ml ethidium bromide (20 mg/ml in TES). The mixture was centrifuged for 40 h in a fixed angle 50-Ti rotor using a Beckman Model L3-50 preparative centrifuge at 42 000 rpm and 19°C. The high density plasmid band, containing supercoiled, covalently closed $ColE_1$-I [34], was collected with the aid of a LKB 12000 Varioperpex peristaltic pump through a narrow glass capillary, inserted through the top of the gradient into the center of the band. The collected $ColE_1$-I fraction was freed of ethidium bromide by extraction with isopropanol, dialyzed against 0.3 M NaCl, 0.005 M EDTA, 0.05 M Tris pH 8.0 and precipitated with 2.2 volumes of reagent grade ethanol. After storage for 12 h at –20°C the precipitate was collected by centrifugation. The $ColE_1$-I preparation is quite pure

at this stage but does still contain some low molecular weight UV-absorbing material, making an additional sucrose gradient centrifugation step necessary. The ethanol precipitate was, therefore, redissolved in 1–3 ml of TES and up to 1 ml of this solution was loaded on top of 27 ml of a linear 5–20% (w/w) gradient of sucrose in 0.3 M NaCl, 0.05 M Tris pH 8.0, 0.005 M EDTA. The sample was centrifuged in a SW 25.1 swinging bucket rotor in a Beckman Model L3-50 centrifuge at 21000 rpm and 4°C for 18 h. Fractions of 0.7–0.8 ml were collected from the gradient with the aid of the LKB 12000 Varioperpex pump through a glass capillary inserted onto the bottom of the gradient tube. The fractions of the $ColE_1$-I peak with $OD_{260} > 1$ were combined, dialyzed, precipitated and the precipitate collected by centrifugation as described above. For each preparation, 2 liters of culture medium were processed with the above procedure.

2.3. Preparation of $ColE_1$-II

$ColE_1$-I (~4 mg) was dissolved in 5–10 ml of 0.05 M NaCl, 0.005 M $MgCl_2$, 0.1 M Tris pH 7.5 and dialyzed against the same buffer for 24 h. DNA'se-I was then added to a concentration of 0.01–0.02 μg/ml and the reaction was allowed to proceed at 0°C until about 50% of the $ColE_1$-I was converted into $ColE_1$-II. The rate of conversion had been determined before in a pilot experiment employing much smaller amounts of $ColE_1$-I DNA (0.1-0.1 mg); the fraction of $ColE_1$-II formed was monitored in the analytical ultracentrifuge. The reaction was stopped by adding a 4–5 fold excess of 0.25 M EDTA over the $MgCl_2$ present in the solution. The forms I and II were then separated by density gradient centrifugation [23], and the bands were collected and processed exactly as described above.

2.4. Preparation of $ColE_1$-III

Linear $ColE_1$-III was prepared by reaction of $ColE_1$-I with the restriction enzyme EcoRI, which cleaves $ColE_1$-DNA in only one position. The reaction was initiated by adding 50 μl of the EcoRI solution to 5 ml of DNA solution (1–2 mg/ml) in 0.1 M Tris pH 7.5, 0.05 M NaCl, 0.005 M $MgCl_2$ and 0.1 mg/ml of BSA. The reaction mixture was left at room temperature (23–25°C) until the reaction was completed (20–30 h) as judged by sedimentation velocity in 0.3 M NaCl, 0.05 Tris pH 8.0, 0.005 M EDTA or gel electrophoresis on agarose slab gels in 0.02 M Na Ac, 0.002 M EDTA, 0.04 M Tris pH 7.8. The reaction was then stopped by addition of excess EDTA, proteins were removed by phenol extraction and the $ColE_1$-III was dialyzed, precipitated and collected by centrifugation as described above.

2.5. Determination of DNA concentration

DNA concentrations were determined from optical density measurements at 260 nm using 1 cm quarz cuvettes after gravimetric dilution of the solution into the range $0.2 < OD_{260} < 0.9$. A Zeiss PMQ II spectrophotometer was used for these measurements and a value $E^{0.1\%}_{1\,cm,260} = 20.4$ was used for the calculation of c. The latter value was determined from orthophosphate content analysis of $ColE_1$-III DNA samples by the method of Morrison [35] (see sect. 3).

2.6. Sedimentation velocity analysis

Sedimentation velocities of the three forms of $ColE_1$-plasmid DNA were measured with a Beckman Model E Analytical Ultracentrifuge equipped with electronic speed control, photoelectric scanner system and multiplex accessory unit. DNA solutions (5–40 μg/ml) were dialyzed exhaustively against 0.2 M NaCl, 0.002 M $NaPO_4$ pH 7.0, 0.002 M EDTA ("Solvent B" of ref. [16]) prior to sedimentation analysis. The cell, fitted with a 12 mm aluminium filled epon double sector centerpiece and quartz or sapphire windows, was filled with the dialyzed DNA solution and the dialyzate solvent. The cells were loaded in either the two-hole An-H or the four-hole An-F titanium rotor. They were centrifuged at rotor speeds varying from 30000 to 44000 rpm at approximately 23°C. The RTIC temperature regulating unit was not used during the run. The cells and rotor were instead kept at the required temperature by adjusting the temperature of the freon cooling fluid to values between 10–16°C. The rotor temperature was constant to within 0.1°C during the run. Cells were scanned at 265 nm at 4 minute intervals. Sedimentation coefficients for the main component in the preparation were obtained from midpoint (the point of maximal dc/dr) analysis of the sedimenting boundaries with the aid of a Hewlett-Packard 9810 A calculator. In addition, weight-average sedimentation coef-

ficients for the whole preparation (including, for instance, a contribution due to dimers in preparations of $ColE_1$-I and $ColE_1$-II) were calculated by the boundary analysis procedure outlined by Schumaker and Schachman [36].

The values obtained were corrected to standard conditions (the viscosity and density of pure water at 20°C) in the usual manner using a value [16] $\phi' = 0.547$ ml/g for the apparent partial specific volume [37].

2.7. Light scattering

Quasielastic and total intensity laser light scattering experiments were performed using a modified Malvern photon correlator (Malvern Molecular Analyzer 4300, Precision Devices and Systems (UK) Ltd., Malvern). A detailed description of this instrument indicating also instrumental modifications and calibration procedures has been reported before [17].

In the quasielastic laser light scattering experiments, the Malvern RR 95 scaling and clipping extender unit was used to compute the prescaled, clipped autocorrelation functions of the scattered light fluctuations [38]. The accumulated result was analyzed in a Hewlett-Packard 9810 A calculator using the cumulants fit method [39]. A single exponential fit with decay time τ extrapolated to forward scattering angle θ ($\theta \rightarrow 0$) gives the translational diffusion coefficient $D_{23,s}$, according to:

$$D_{23,s} = 1/\tau q^2, \qquad (1)$$

where q is the scattering vector, $q = (4\pi n/\lambda) \sin(\theta/2)$, λ is the wavelength in vacuo and n the refractive index of the medium and $D_{23,s}$ refers to the experimental conditions (23°C, 0.2 M NaCl, 0.002 M $NaPO_4$ pH 7.0, 0.002 M EDTA). The angular dependence of the correlations of the scattered light was measured to scattering angles as low as 7°.

Total intensity light scattering experiments, giving the weight-average molecular weights and the z-average radii of gyration and second virial coefficients for the various forms of the plasmid DNA, were performed at various scattering angles down to 7° in the Malvern instrument. Benzene was used as a standard for calibration of the absolute intensities. The Rayleigh ratios of benzene for the vertically polarized mercury lines are $R_v(90) = 22.4 \times 10^{-6}$ at 546.1 nm and $R_v(90) = 65.3 \times 10^{-6}$ at 435.8 nm [40]. The corresponding value for the Argon ion laser wavelength used in the Malvern instrument was calculated by interpolation to be $R_v(90) = 29.9$ at 514.5 nm using expressions derived by Cohen and Eisenberg [41]. The total intensities of the scattered light, measured at different scattering angles and DNA-concentrations at 23°C were plotted according to the method of Zimm [42]. The data obtained by extrapolation at constant scattering angle to zero concentration ($c = 0$) or by extrapolation at constant concentration c to zero scattering angle ($\theta = 0$) were analyzed by the familiar equations

$$\left(\frac{Kc}{\Delta R}\right)_{\theta=0} = \frac{1}{M_w} + 2A_2c + \ldots, \qquad (2)$$

$$\left(\frac{Kc}{\Delta R}\right)_{c=0} = \frac{1}{M_w P(\theta)} = \frac{1}{M_w}(1 + q^2R_{gz}^2/3 + \ldots), \qquad (3)$$

where all of the symbols have their usual meaning [18, 43]. For the refractive index increment at 514.5 nm we used 0.168 ml/g [17].

All DNA stock solutions used for light-scattering measurements were dialyzed against 0.2 M NaCl, 0.002 M $NaPO_4$ (pH 7.0) and 0.002 M EDTA and clarified by filtration through 0.45 μm Millipore filters into carefully cleaned, dust-free cuvettes. Dilutions with solvent were made by weight and DNA concentrations determined spectrophotometrically after completion of the measurements as described below.

2.8. Viscometry

Viscosity measurements were made in two entirely different types of viscometers. We used a Zimm–Crothers low shear rotating viscometer [44] manufactured by Beckman Instruments, fitted with a Kel-F rotor with a rate of shear of approximately 1.4 s^{-1} for the solvent, and less for the DNA solutions, a value low enough to ensure Newtonian behavior of the DNA solutions measured in this study [45]. Water maintained at 23.0 ± 0.02°C was circulated through the stator-jacket of the viscometer. Rotor times (about 21 s/revolution) for the solvent (0.2 M NaCl, 0.002 M $NaPO_4$ pH 7.0, 0.002 M EDTA) were usually reproducible to within 0.2%. The flow in this viscometer is of the Couette type and the reduced specific viscosity is calculated from the rotation time (t) of the rotor in

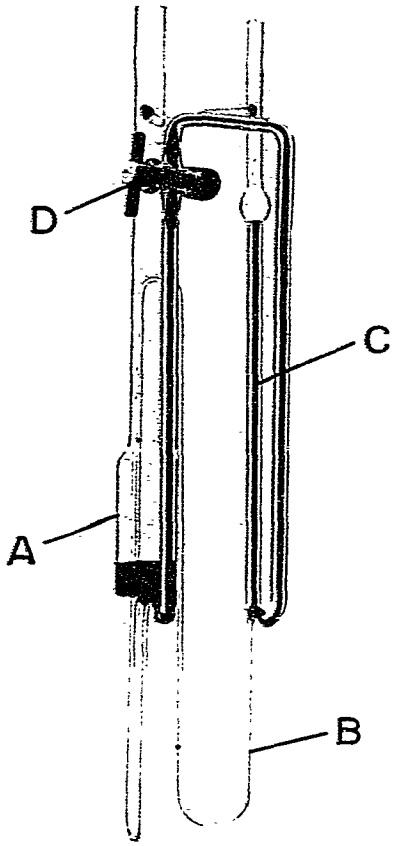

Fig. 1. Variable level viscometer (see text).

the solution, the rotation time (t_0) in the solvent, and the DNA concentration (c in g/ml) according to:

$$\eta_{sp}/c = (t - t_0)/t_0 c. \quad (4)$$

In addition, viscosity measurements were made with a capillary viscometer with continuously variable pressure head [46,37]. The flow in this viscometer is of the Poiseuille type. The instrument made in this laboratory (fig. 1) has a sample reservoir A (ϕ = 2.5 cm) connected via a 93 cm long, coiled capillary B (ϕ = 0.05 cm) to a precision bore measuring tube C (ϕ = 0.2 cm). The menisci in both the sample reservoir and the precision bore capillary are under atmospheric pressure. The relaxation of the meniscus of the sample liquid from height h to its gravitational equilibrium level h_0 ($h > h_0$) was recorded by determining the times t at which the liquid meniscus passed through the horizontal cross-hair of a cathetometer, preset accurately at known height-levels. We studied height differences Δh between 13 and 0.3 cm (maximum rate of shear at capillary wall between 190 and 4.3 s^{-1} for the solvent). The equilibrium level h_0 was determined by opening a bypass (stopcock D) connecting the sample reservoir A and precision bore tube C. The data, when plotted as $\log(h - h_0)$ versus t, yielded straight lines (over the whole range of driving pressures) with slopes m and m_s for solution and solvent, respectively. These slopes, calculated with a linear regression analysis program were combined with the measured DNA concentration (c in g/ml) to give the reduced specific viscosity according to:

$$\eta_{sp}/c = (m_s - m)/mc. \quad (5)$$

The viscometer was kept in a water bath at (23.0 ± 0.02)°C during measurement. All solutions for viscometry were made dust-free by filtration through 0.45 μm Millipore filters.

The $ColE_1$-I sample used for viscosity measurements was repurified by ethidium bromide-CsCl density gradient centrifugation immediately prior to the viscosity study. The plasmid DNA was then run through a column (1.5 × 25 cm) packed with Sephadex-G25 (1.5 × 15 cm) with a top layer of Dowex 50W (1.5 × 6 cm) and equilibrated with 0.2 M NaCl, 0.002 M $NaPO_4$ pH 7.0, 0.002 M EDTA. The supercoiled $ColE_1$-I sample could be freed of ethidium bromide and CsCl and equilbrated with the above buffer in about 30 min. Viscosity measurements on this sample, which may be considered free of $ColE_1$-II, were started immediately after isolation.

2.9. Electron microscopy

Electron micrographs were taken using a Philips EM-300 electron microscope at 60 kV with a nominal grid to plate magnification of 17000 in the bright-field mode. Pictures were recorded on Kodak electron image plates. The DNA molecules, spread by the protein monolayer technique of Kleinschmidt [47] were picked up on

parlodion grids, positively stained with uranyl acetate and rotary shadowed using Pt-Pd. For contour length determinations of ColE$_1$-III, the plates were printed on 30 × 24 cm sheets (an enlargement of approximately 3 times) at one session of the photographic enlarger, to ensure uniform magnification. The contour lengths of all of the molecules for which the contour was clearly defined (about 90%) were measured (in arbitrary units) using an acoustically operated SAC Graf/Pen (Scientific Accessories Corp., Southport, Conn.) interfaced to a PDP-15 computer. This instrument measures contour lengths with a precision of 2% (standard deviation of multiple length measurements on a single molecule).

3. Results

3.1. Purification of the Plasmid DNA

The ColE$_1$-plasmid is a particularly suitable molecule for the studies presented here, as large quantities (10–20 mg) can conveniently be obtained. Since it is most essential that the chromosomal DNA be nearly quantitatively removed before ethidium bromide-CsCl density gradient centrifugation, we decided to use the lysis procedure of Clewell and Helinski [21–23] as modified by Guerry et al. [33]. Practically all of the chromosomal DNA was precipitated by this procedure, provided the viscous suspension was handled very gently during lysis. Subsequent density gradient centrifugation was nevertheless considered a useful purification step, leading to the removal of the last remaining chromosomal DNA-fragments and of open circular ColE$_1$-II banding together at lower density than the main band containing the supercoiled ColE$_1$-I plasmid [34]. We did not use the material from the low density band for physical measurements, in view of the small amount of chromosomal DNA impurity and because the ColE$_1$-II in this band may have protein covalently attached [22–26]. In addition, density gradient centrifugation separates ColE$_1$-I from high density ribonucleic acids and low density proteins, which form a solid film at the top of the gradient. Subsequent sucrose gradient centrifugation proved very effective in removing slowly sedimenting material. The ColE$_1$-I plasmid sedimented as a single broad peak, which included small amounts of ColE$_1$-II and dimers (see below). These can in principle be resolved by sucrose gradient centrifugation (e.g. ref. [21], fig. 6), provided sufficiently small samples are loaded, giving pure, monomeric ColE$_1$-I. However, as we needed large quantities for our studies, quantitative separation was not considered feasible and was not attempted. The total yield from 2 ℓ of culture medium varied from 3–8 mg of ColE$_1$-I. The reasons for this variability are not clear.

Spectral analysis was used occasionally to monitor the quality of the resulting product. By combining absorbancy values measured at 12 wavelengths (from 235 nm to 290 nm at 5 nm intervals) with tabulated numerical data [48] values for ϵ(P), the molar phosphorus extinction coefficient and ϕ, the fraction of AT-basepairs, can be obtained. Calculated values for ϵ(P) and ϕ varied by less than 1% and 8%, respectively, for different preparations. We obtained an AT content of 52% and an average ϵ(P) = 6530 liter mole^{-1}cm^{-1} at 260 nm but this value may be systematically in error by as much as 5% [48]. We relied, therefore, on direct phosphorus analysis [35] for determining ϵ(P). The results of nine determinations (OD_{260} = 0.15 to 1.2) indicated a linear relationship between the amount of DNA (in OD_{260} units) and the phosphorus content of the sample. Linear regression analysis calculation of the slope gave ϵ(P) = (6770 ± 90) liter mole^{-1}cm^{-1} at 260 nm which, when combined with an average nucleotide molecular weight of 331 for the sodium salt, leads to $E^0_{1\,cm,260}$ = (20.4 ± 0.3). As spectral analysis does not indicate significant absorbancy differences for the various forms of ColE$_1$-plasmid DNA, this value has been used throughout for the calculation of weight concentrations.

Repeated phenol extraction of any of the plasmid-DNA samples used did not result in spectral changes, monitored by calculating ϵ(P), indicating the DNA samples to be free of protein, at least in the limit of sensitivity of the spectral method.

3.2. Electron microscopy

A few representative fields of samples of ColE$_1$-I, II and III, spread by the Kleinschmidt technique [47] are shown in fig. 2. All three forms appear homogeneous under the electron microscope. Small fragments and long strands of chromosomal DNA, which can be found in unpurified preparations, are absent in the puri-

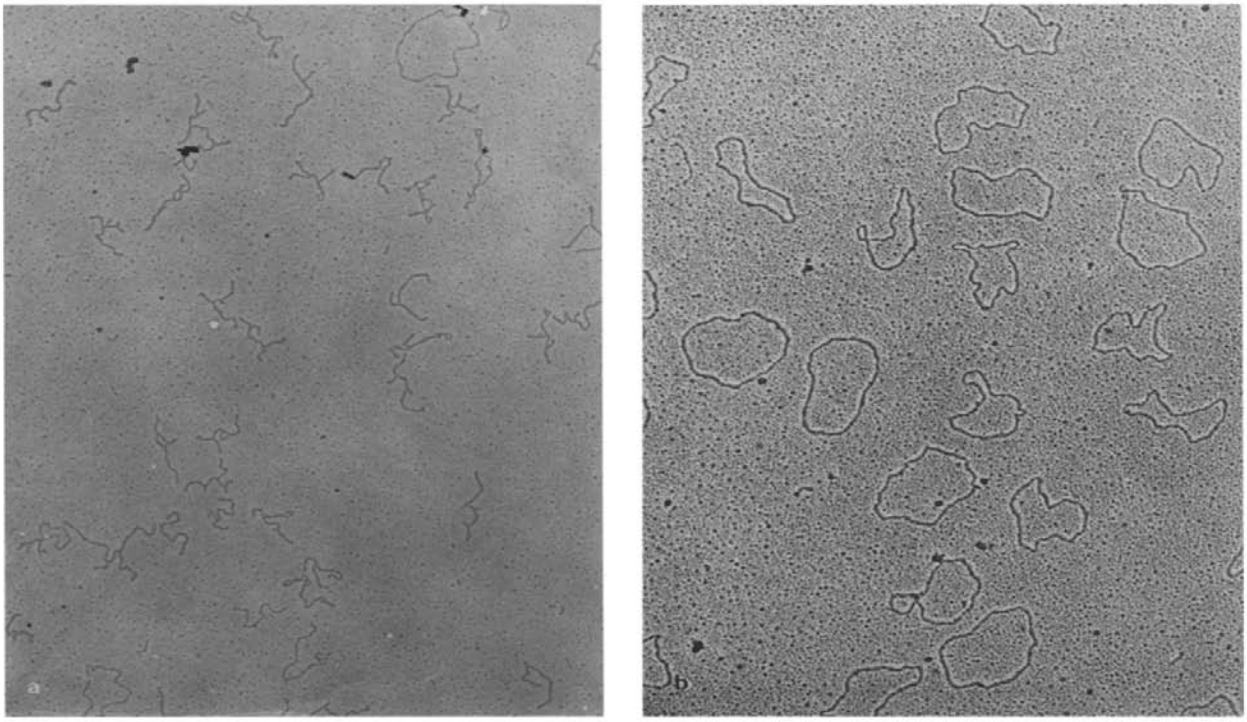

(a) (b)

Fig. 2. Representative electron micrograph fields for $ColE_1$-plasmid DNA showing the supercoiled form I (a), the open circular form II (b) and the linear form III (c). The bars indicate 0.5 μm. (Fig. 2(c) on next page)

fied samples. Forms I and II do generally show a slight cross-contamination (see fig. 2a in which at least one open circle appears) and are partly present as dimers. Most of these are of the concatenated type only a few circular dimers being present (see ref. [49] for electron micrographs of concatenated dimers of $ColE_1$-DNA). The following weight composition was derived for a typical sample of $ColE_1$-II from examination of 260 molecules: $ColE_1$-II, monomer 88%; $ColE_1$-I, monomer 3%; $ColE_1$-III, monomer 0.4%; $ColE_1$-II, catenated dimer 8%, $ColE_1$-II, circular dimer 0.7%. The percentage of catenated dimers may have been overestimated, as they are difficult to distinguish from accidentally superimposed monomeric molecules. Reliable estimation could be achieved by spreading different concentrations of DNA on the grid and extrapolating to infinite dilution. This has not been attempted, however. A simplified representation of the results is given in table 1, together with data derived from boundary analysis.

The $ColE_1$-III preparations appear particularly homogeneous and a length-histogram, including 300 molecules, is shown in fig. 3. The length distribution is approximately Gaussian with a relative standard deviation $\sigma_L = 4.2\%$. Noting that this σ_L-value includes an rms-error of 2% in the measurement of the relative contour-length, we conclude that the actual distribution of lengths on the grid is characterized by $\sigma_L = 3.8\%$. Hence all of the molecules have a very similar, if not a unique contour length. The length-dispersity can also be expressed by the ratio $(\bar{M}_w/\bar{M}_n) = (\Sigma_i N_i L_i^2/\Sigma_i N_i L_i)$, which is equal to 1.0011 for the distribution shown in fig. 3. In comparison, the best calf-thymus fractions obtained in this laboratory have a $\bar{M}_w/\bar{M}_n = 1.04$ [16]. It thus follows that no polydispersity corrections are

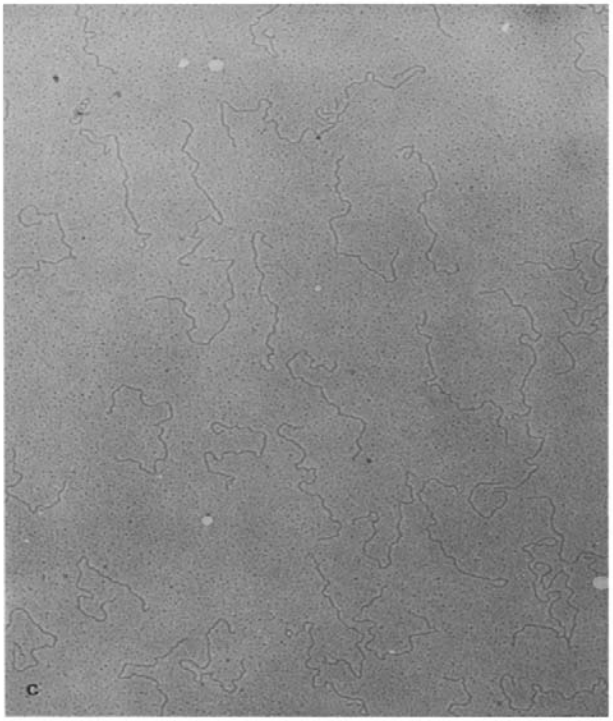

(c)

necessary of physical data obtained for form III, whereas small corrections may be applied in the case of forms I and II.

3.3. Sedimentation velocity

Representative tracings of scans obtained during the course of sedimentation velocity experiments for either $ColE_1$-I, $ColE_1$-II or $ColE_1$-III are shown in fig. 4 (inserts), together with the weight distribution of sedimentation coefficients obtained by boundary analysis [36]. As expected on the basis of the electron microscopy results, a single narrow peak is found to represent the sedimentation coefficient distribution of $ColE_1$-III. In the case of $ColE_1$-I monomeric $ColE_1$-II and dimers sediment at the trailing and leading edges of the main boundary, respectively. The material sedimenting ahead of the main boundary for $ColE_1$-II represents both monomeric $ColE_1$-I and dimers. The weight composition that can be derived from boundary analysis for forms I and II is given in table 1. In the case of $ColE_1$-I a well-resolved boundary for the supercoiled concatenated dimer was observed occasionally. The weight fraction of $ColE_1$-II in $ColE_1$-I samples is only about 3% at the conclusion of the purification procedure. As a single nick in one of the DNA-strands is sufficient to cause relaxation to $ColE_1$-II this percentage rises slowly when solutions are kept for several days. The 7% $ColE_1$-II listed in table 1 is the time-average fraction in the $ColE_1$-I samples pertaining to the light scattering experiments described below.

Table 1
Weight composition of typical samples of $ColE_1$-I and $ColE_1$-II plasmid DNA

$ColE_1$	Method	Composition
I	boundary analysis	81% monomer I, 7% monomer II, 12% dimers
II	boundary analysis	88% monomer II, 12% monomer I + dimer
II	electron microscopy	88% monomer II, 3% monomer I, 9% dimers

Sedimentation coefficients, obtained from the rate of movement of the main boundary (see fig. 4; "midpoint-analysis"), corrected to standard conditions are shown in fig. 5 at various DNA concentrations. It is seen that $s_{20,w}$ decreases only slightly with increasing concentration in the range 5—40 μg/ml. Values $s^0_{20,w}$, extrapolated to zero concentration, are presented in table 2, column c. As $ColE_1$-I and $ColE_1$-II are clearly the main components in their respective preparations and the boundaries for all three forms are of narrow width, the values $s^0_{20,w}$ must closely approximate the true values for the pure forms. This is demonstrated by the data in table 2, where the weight-average sedimentation coefficient for $ColE_1$-III is seen to equal the value obtained by midpoint-analysis. Values $\langle s_{20,w}\rangle_w$, obtained from boundary analysis at a particular DNA concentration, were corrected to zero concentration by using the dependence of $s_{20,w}$ on c as in fig. 5. The difference between $s^0_{20,w}$ and $\langle s^0_{20,w}\rangle_w$ is rather small in the case of $ColE_1$-I, due to partial cancelling of dimer and $ColE_1$-II monomer contributions (see fig. 4). This difference is larger in the case of $ColE_1$-II, as the small amounts of $ColE_1$-I and dimers in the preparation

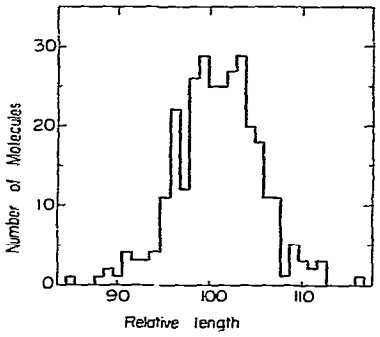

Fig. 3. Contour length histogram for linear ColE$_1$-III plasmid DNA. The lengths (relative units) of 300 molecules are represented in the histogram.

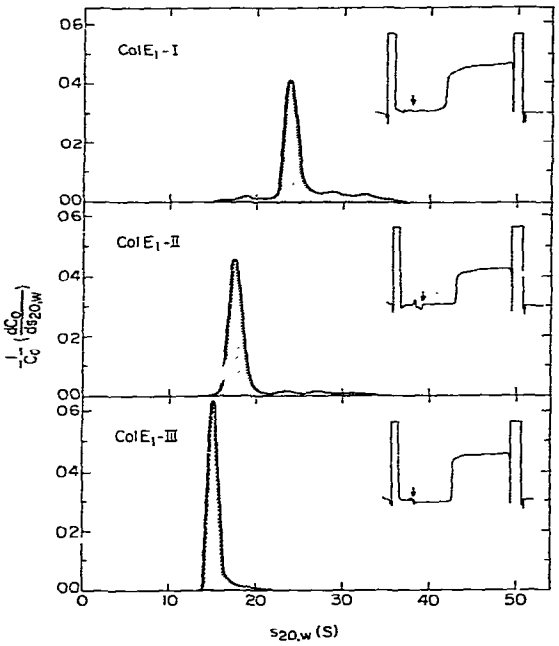

Fig. 4. Representative scans (inserts) and weight distributions of sedimentation-coefficients for the three conformational forms of ColE$_1$-plasmid DNA. The arrow in the scans indicates the meniscus; sedimentation is from left to right at 44,000 rpm, at approximately 23°C, in 0.2 M NaCl, 0.002 M $NaPO_4$ pH 7.0 and 0.002 M EDTA. The cells were scanned at 265 nm at the following effective sedimentation times: 26.6 min for ColE$_1$-I, 29.0 min for ColE$_1$-II and 35.7 min for ColE$_1$-III. The normalized sedimentation coefficient distribution was obtained from the scans according to the procedure of Schumaker and Schachman [36].

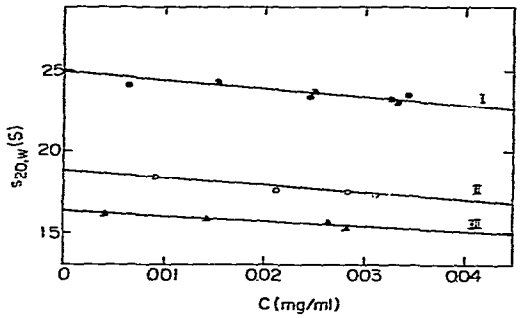

Fig. 5. Dependence of the corrected sedimentation coefficient ($s_{20,w}$) on concentration for the three forms of ColE$_1$-plasmid.

do both increase the average $\langle s_{20,w} \rangle_w$. For diffusion coefficient measurements exactly the opposite may be expected: a significant decrease from the true value for ColE$_1$-I, as both the small amount of ColE$_1$-II and of dimers tend to decrease the average, while in the case of ColE$_1$-II a partial cancelling of contributions is likely to occur.

Values $s^0_{23,s}$ for the sedimentation coefficient under the actual experimental conditions (23°C, 0.2 M NaCl, 0.002 M $NaPO_4$ pH 7.0, 0.002 M EDTA) can be obtained by multiplication of the data in table 2 by the constant factor $F = 1.039$.

3.4. Diffusion coefficients

Translational diffusion coefficients for the three conformational forms of the plasmid DNA were determined by quasielastic laser light scattering. The autocorrelation function of the fluctuations in the intensity of the scattered light was determined as function of the scattering angle θ and fitted to a single exponential with decay-time τ. Both translational and rotatory diffusion and internal relaxations may contribute to the auto-correlation. However, at angles $\theta < 30°$, the fitted single exponential can be attributed to purely translational diffusion and obeys eq. (1). This is apparent from the constant value obtained for $D_{20,w}$ from the single exponential fit in the range $7° < \theta < 30°$ (fig. 6). At angles $\theta > 30°$ the value for the apparent $D_{20,w}$ deduced from the fit rises indicating that other contributions come into play. This effect was found for all three forms (fig. 6) and has been previously described by Jolly and Eisenberg [17] for a linear calf-thymus DNA

Table 2
ColE$_1$-plasmid DNA, physical chemical properties of three conformational forms in solution

	a	b	c	d	e	f	g	h	i	j
ColE$_1$	$\bar{M}_w \times 10^{-6}$	$\bar{R}_{gz}$	$s^0_{20,w}$	$\langle s^0_{20,w}\rangle_w$	$\langle D^0_{20,w}\rangle_z \times 10^8$	$\bar{M}_{s,D} \times 10^{-6}$	$A_2 \times 10^4$ mole/ml/g^2	$[\eta]$	k	$\beta \times 10^{-6}$
I	4.59	103.5	(24.5 ± 0.3)	25.4	2.89	4.69	0.70	(788 ± 23)	(0.70 ± 0.19)	2.39
II	4.15	134.2	(18.8 ± 0.1)	20.1	2.45	4.37	4.8	(1421 ± 22)	(0.68 ± 0.05)	2.49
III	4.30	186	(16.3 ± 0.3)	16.3	1.98	4.39	5.4	(2605 ± 27)	(0.55 ± 0.02)	2.40

a) Weight average molecular weight from total intensity light scattering (TILS).
b) z-Average radius of gyration from TILS (nm).
c) Sedimentation coefficient from midpoint-analysis, corrected to standard conditions and extrapolated to zero concentration (S).
d) Weight average sedimentation coefficient from boundary analysis; corrected and extrapolated (S).
e) z-Average diffusion coefficient from quasielastic laser light scattering; corrected and extrapolated ($cm^2 s^{-1}$).
f) Molecular weight from sedimentation and diffusion coefficients as in columns d and e.
g) z-average second virial coefficient from TILS (mole ml g^{-2}).
h) Intrinsic viscosity (ml g^{-1}).
i) Huggins' constant, eq. (7).
j) Mandelkern-Flory parameter in 0.2 M NaCl, 0.002 M $NaPO_4$ pH 7.0, 0.002 M EDTA at 25°C.

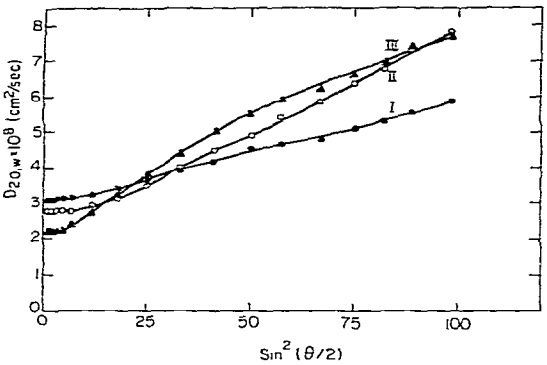

Fig. 6. Apparent translational diffusion coefficients ($D_{20,w}$) obtained from a single exponential fit to the autocorrelation function (eq. (1)) as function of the scattering angle θ for the three forms of ColE$_1$-plasmid DNA. Experimental conditions: 23°C, 0.2 M NaCl, 0.002 M $NaPO_4$ pH 7.0, 0.002 M EDTA. DNA concentrations: I, 0.275 mg/ml; II, 0.198 mg/ml, III, 0.258 mg/ml.

fraction of similar average molecular weight ($\langle M_w \rangle = 3.7 \times 10^6$) and interpreted as an intramolecular relaxation time. We will present a detailed analysis of the correlation curves at higher scattering angles in a separate contribution. Here we note that the increase in the apparent $D_{20,w}$ with scattering angle is much smaller for the supercoiled ColE$_1$-I than for either ColE$_1$-II or ColE$_1$-III.

Values for the translational diffusion coefficients $D_{20,w}$ obtained at low angles ($0 < \theta < 30°$) are plotted as function of DNA concentration in fig. 7. The extrapolated values, $D^0_{20,w}$, are listed in table 2 and show the same trend as the sedimentation coefficients: $D^0_{20,w}$ is largest for ColE$_1$-I, much smaller for ColE$_1$-II and smaller again for ColE$_1$-III reflecting an increased hydrodynamic volume and translational frictional coefficient. The value listed for form III (table 2) is unambiguous, but those for forms I and II contain contributions due to contaminants discussed above. The average measured by quasielastic linear light scattering equals approximately the z-average $\langle D^0_{20,w} \rangle_z$. This value, when combined with the weight-average sedimentation coefficient $\langle s^0_{20,w} \rangle_w$, gives the weight average molecular weight by means of the Svedberg equation, which for amonodisperse solute takes the form:

$$M = RT s^0 / D^0 (1 - \phi' \rho), \qquad (6)$$

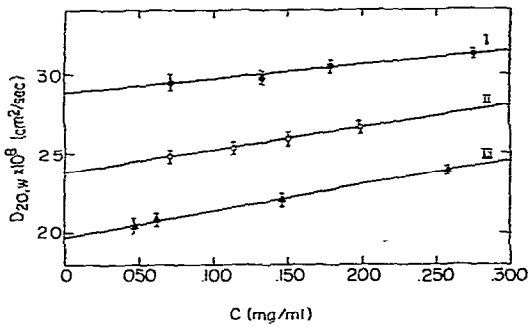

Fig. 7. Dependence of the corrected diffusion coefficient ($D_{20,w}$) on concentration for the three forms of ColE$_1$-plasmid DNA.

where ϕ' is the apparent specific volume of the macromolecular solute [37], ρ is the density of the solvent and R and T have their usual meaning. Eq. (6) is likely to hold as well for the narrowly disperse (see fig. 4) solutions investigated here. Inserting the average quoted above into eq. (6) and using $\phi' = 0.547$ ml g^{-1} leads to the average molecular weights $M_{s,D}$ shown in table 2, column f. These are in good agreement with the weight average molecular weights from total intensity light scattering (table 2, column a).

3.5. Total intensity light scattering

The conventional Zimm plots for linear conformational form III (over a wide angular range) and the circular form II (at low angles only) are shown in figs. 8 and 9. In fig. 10 we show the function $P^{-1}(\theta)$ (eq. (3)) extrapolated to $c = 0$, against $\sin^2(\theta/2)$ for small angles only. It has been demonstrated (fig. 6, ref. [43]) that for the evaluation of the radius of gyration R_g by eq. (3), it is necessary for $X \equiv q^2 R_g^2$ to be smaller than 0.3, for the experimental points to be on the Zimm limiting slope; for a linear DNA molecule with $M \sim 4 \times 10^6$ and $R_g \sim 200$ nm at $\lambda \sim 500$ nm, this means scattering angles $\theta < 12°$. For larger values of X the complete particle scattering factor $P(\theta)$ rather than the first term in the linear Zimm expansion in q^2 (eq. (3)) has to be taken. Fortunately (fig. 6; ref. [43]) up to values X of about 2, $P^{-1}(\theta)$ of random coils and of rigid rods are indistinguishable. Therefore, in the example quoted above, the analytical function of Debye for $P(\theta)$ of gaussian coils can be used for the calcula-

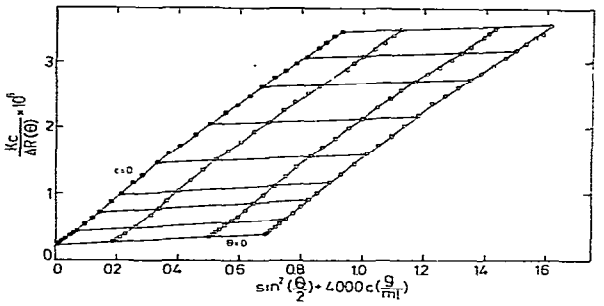

Fig. 8. Total intensity light scattering Zimm plot for ColE$_1$-plasmid DNA Form II at low scattering angles. Experimental conditions as in fig. 6.

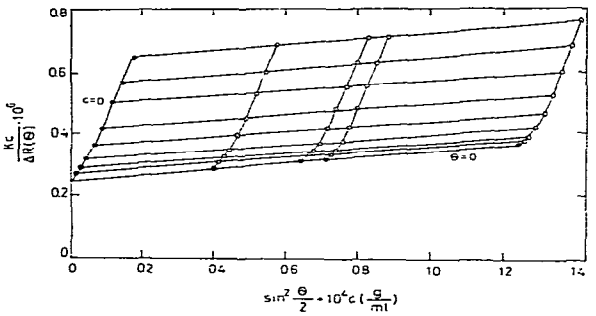

Fig. 9. Total intensity light scattering Zimm plot for ColE$_1$-plasmid DNA Form II at low scattering angles. Experimental conditions as in fig. 6.

tion of R_g from the experimental scattering envelope up to $\theta = 30°$. (Deviations from linearity in this range in the theoretical curves cannot be experimentally determined). This procedure was followed in this work for the evaluation of R_g of the linear form III, from the angular dependence of scattering (upper set of data, fig. 10). A value R_g = 186 nm was derived from this analysis. Use of Zimm's expansion, rather than the complete $P(\theta)$ function would lead up to about 10% overestimation in the values of R_g. The experimental values, up to $X < 7$, closely follow the gaussian coil model. We shall see below that this is to be expected from scattering theory of stiff coils and deviations from this behavior occur at higher values of X. The molecular weight, R_g and virial coefficients for all three forms examined are given in table 2.

Light scattering results for form II (middle set of data, fig. 10) have been analyzed by a calculation of Casassa [50] of the statistical properties of flexible Gaussian ring polymers. A distinctly smaller value R_g = 134.2 nm is obtained (curve d, fig. 10). The agreement with the initial Zimm slope extends to slightly higher values of the scattering angle; X_{max} is below 4 and deviations from the Gaussian coil model are not likely to be significant. Finally (lower set of data, fig. 10) the scattering for the supercoiled form I yields R_g = 103.5 and analysis by the limiting Zimm slope becomes feasible. Curve f has been drawn following a calculation of Jolly and Campbell [30] for a Y shaped supercoil with equal arms, yet at the maximum limit of about 2 of the value of X examined, analysis of the shape of the scattering curves is not likely to distinguish between various molecular supercoiling models. For this purpose analysis over a wider range of scattering vectors will be reported elsewhere.

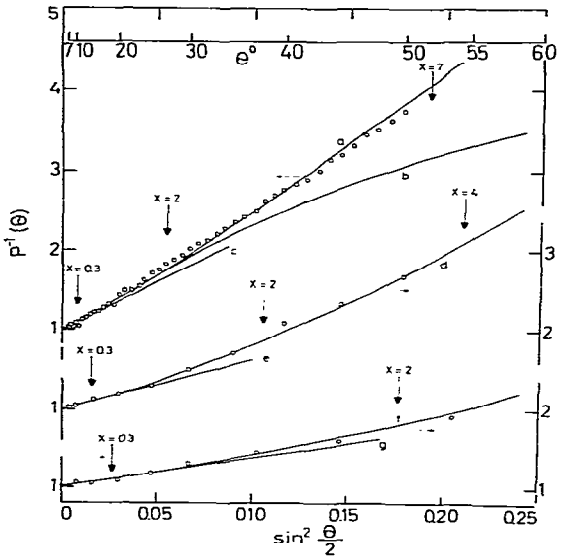

Fig. 10. Angular dependence at low angles of scattering of ColE$_1$-plasmid DNA, Form I, supercoiled (lowest set of data); Form II, circular rings (middle set of data); Form III, top set of data, at low angles of scattering. Theoretical curves a) gaussian coils R_g = 186 nm; b) thin rods, same R_g as (a); c) Zimm limiting slope, same R_g as (a); d) gaussian ring [50], R_g = 134.2 nm; e) Zimm limiting slope, same R_g as (d); f) Supercoiled Y with equal arms [30] R_g = 103.5 nm; g) Zimm limiting slope, same R_g as (f). Experimental conditions as in fig. 6.

An unambiguous measurement of the monomer molecular weight of the $ColE_1$-plasmid is possible only with the linear form $ColE_1$-III, and the average of 4.34×10^6 (see table 2, M_w and $M_{s,D}$ for $ColE_1$-III) is the best value for this molecular weight. The values obtained for M_w and $M_{s,D}$ of $ColE_1$-II are rather similar, despite the fact that there is a non-negligible fraction of concatenated dimers in the sample (table 1). The fraction of dimers in the given $ColE_1$-II sample may have been overestimated, otherwise the agreement must be regarded as fortuitious. Another tantalizing possibility (unless experimental inaccuracy is the trivial explanation) is that dimers topologically concatenated but otherwise free to move independently contribute as monomers, rather than dimers when examined in solution. The molecular weights found for $ColE_1$-I are indeed significantly higher about 4.6×10^6 (table 2, columns a and f) indicative of a dimer contribution. The observed molecular weights fall only slightly short of the value expected for a sample with 10% (w/w) of dimers ($M_w = 4.77 \times 10^6$).

3.6. Viscosity

The viscosities of solutions of linear $ColE_1$-III plasmid DNA were determined at 23°C using both the Zimm–Crothers and the capillary viscometer described in sect. 2.8. Both viscometers operate at low shear rates. Some of the flow curves, obtained with the capillary viscometer and plotted as $\log(h\text{-}h_0)$ versus t, are shown in fig. 11. The linearity of the plots at all concentrations of the $ColE_1$-III plasmid indicates that the flow is newtonian in the rate of shear range (about 4.3 to 190 s^{-1}) in which this viscometer is operating (see sect. 2.8). The slopes of the lines in fig. 11, which are proportional to the reciprocal of the viscosity of the solution, decrease with increasing concentration of the $ColE_1$-III plasmid. The reduced specific viscosities, calculated from these slopes according to eq. (5), are shown in fig. 12, together with the data for $ColE_1$-III obtained by Zimm–Crothers viscometer (rate of shear about 1.4 s^{-1}). As the two viscometers are basically different in their design and mode of operation (see sect. 2.8) the good agreement between the two sets of data for $ColE_1$-III indicates that both instruments are free of systematic instrumental errors.

The non-Newtonian flow of dilute aqueous solutions of DNA decreases sharply with decreasing molecular

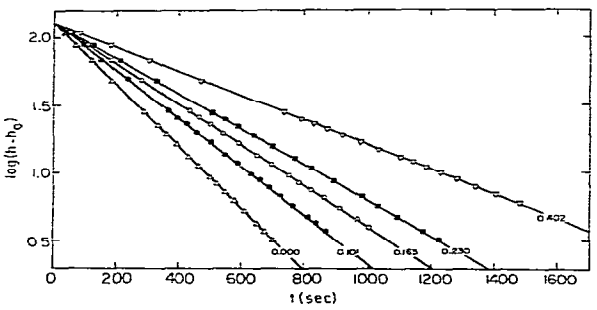

Fig. 11. Flow curves, plotted as $\log(h\text{-}h_0)$ versus time t, obtained with the capillary viscometer with continuously variable pressure head for solutions containing various concentrations of $ColE_1$-III. Experimental conditions as in fig. 6.

weight. It is now known that molecular weights of DNA were grossly underestimated previously and M of samples of DNA used in our early study [45] were probably much higher than the values ~6×10^6 given. It is therefore not surprising that the $ColE_1$-III samples exhibits Newtonian behavior to a fairly high rate of shear, and gratifying that a precise determination of intrinsic viscosity is feasible for the study of conformational changes. Any structure more compact than the $ColE_1$-III sample studied can therefore be examined in the instruments described without worry with respect to non-Newtonian behavior.

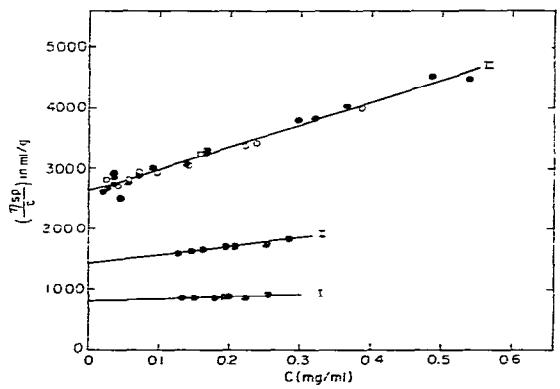

Fig. 12. Reduced specific viscosities (η_{sp}/c) as function of concentration c for the three forms of $ColE_1$-plasmid DNA. Open circles: capillary viscometer. Closed circles: Zimm-Crothers viscometer. Experimental conditions as in fig. 6.

Measurements for $ColE_1$-I and $ColE_1$-II plasmid DNA were carried out using the Zimm–Crothers viscometer only. Different samples of $ColE_1$-III plasmid DNA gave reproducible results indicating a constant quality of the samples used, since the reduced specific viscosity is very sensitive to small amounts of extraneous DNA or protein impurities.

The η_{sp}/c data in fig. 12 were fitted by a linear least squares program and the intrinsic viscosities $[\eta]$ and the Huggins' constants k calculated from the relation

$$\eta_{sp}/c = [\eta] + k[\eta]^2 c \qquad (7)$$

and tabulated in table 2. The data shown for $ColE_1$-II in fig. 12 have been obtained using the same sample as that used in light scattering. A separately prepared sample yielded $[\eta] = (1395 \pm 25)$ ml g^{-1} in good agreement with the tabulated value. However, the data for this sample showed a stronger concentration dependence, $k = 1.11$. This value for the Huggins' constant k appears anomalously high and these data are therefore not presented in fig. 12.

4. Discussion

Theoretical aspects concerning the dimensions of ring macromolecules have been analyzed very early [51,52] even before such molecules were experimentally available. The discovery that natural macromolecules, such as deoxyribonucleic acids from the bacteriophage ϕX 174 [53] and from a polyoma virus [54] occur in closed rings provided additional justification for a continued study of this topic. Circular, and also supercoiled macromolecules, are quite ubiquitous [55] and have in recent years been subject to constant investigation [14]. In the area of theory Casassa [50] examined a "string-of-beads" statistical model for flexible chain polymer rings for which he considered the intramolecular excluded volume, the second virial coefficient and the angular dependence of scattering of the unperturbed molecule. Hydrodynamic properties (viscosity and sedimentation) were calculated by Bloomfield and Zimm [56] and Fukatsu and Kurata [57] for related models. The sedimentation coefficients of linear and cyclic Kratky–Porod wormlike coils were evaluated by Gray, Bloomfield and Hearst [58] and their scattering properties (as well as those of hypothetical supercoiled structues) were calculated by Jolly and Campbell [30]. More recently Fujii and Yamakawa [59] calculated moments and transport coefficients of wormlike rings without excluded volume, following the earlier work of Yamakawa and Fujii [60] of light scattered from linear wormlike chains.

A by no means exhaustive list of experimental results follows. The ratio of the intrinsic viscosities of the linear and circular forms of λ-DNA have been determined by Douthard and Bloomfield [61] as a function of ionic strength, and the viscosity and sedimentation of double-stranded ϕX174 DNA has been measured by Opschoor et al. [62] (Table 3 of ref. [62] lists earlier work on the sedimentation coefficients of circular double-stranded SV-40, Polyoma RF ϕX174, Papilloma and λ-DNA). The sedimentation behavior as a function of superhelix density of covalently closed cyclic DNA's from E. coli (Plasmids and phages) and of SV-40 DNA have been determined by Wang [63] and by Upholt et al. [64], respectively. Light scattering and hydrodynamic properties of linear and circular bacteriophage λ-DNA have been determined by Dawson and Harpst [65] and light scattering of the supercoiled and circular relaxed form of ϕX174 DNA by Jolly and Campbell [30,31].

The theoretical problems associated with the comparison of the behavior of coiling ringlike and linear chains have only been partially solved. It is reasonably straightforward to consider the conformational properties of Gaussian linear chains and rings (obtained by closure of the chain extremities) without excluded volume [50–52]. In double-stranded DNA though non-ideality enters because of the inherent stiffness of the double helix chain, excluded volume effects of the usual type (in particular for very high molecular weight DNA) and also due to polyelectrolyte charge repulsions. For ideal solutions of linear gaussian chains consisting of N segments of length b the mean-square nonperturbed distance $\langle R^2\rangle_0$ between ends is equal to

$$\langle R^2\rangle_0 = b^2 N \qquad (8)$$

and for non-ideal linear chains

$$\langle R^2\rangle = b^2 N^{1+\epsilon}, \qquad (9)$$

where the chain expansion parameter ϵ expresses non-ideality due to both excluded volume and chain stiff-

ness. On the basis of this and similar considerations, it is now possible to calculate approximately $[\eta]$, s, A_2, R_g and other quantities for both linear and cyclic chains; coil stiffness is best expressed by use of the Kratky–Porod wormlike chain. The parameter ϵ may depend on ionic strength, temperature, chain length and other parameters — short and long range interactions are not easily separable. Fukatsu and Kurata [57] have compared the properties of rings and linear chains at equal values of z (rather than at equal values of ϵ)

$$z = (3/2\pi b^2)^{3/2}\beta N^{1/2}, \qquad (10)$$

where z is a purely long-range excluded volume parameter and β is the volume pair-wise excluded by chain segments. The ratios of the quantities referring to rings and linear chains can be calculated in dependence of either ϵ or z. Fortunately this dependence is moderate although it has for instance not been possible to establish unambiguously experimentally [61] or to prove theoretically whether the ratio $[\eta]_C/[\eta]_R$ of $[\eta]$ for linear coils C or circular rings R should increase slightly or decrease with increasing non-ideality; with $\epsilon_C = 0$, $[\eta]_C/[\eta]_R$ was calculated to be [56] about 1.55 and about 1.65 at $\epsilon_C = 0$ 2. The ratio s_C/s_R of the sedimentation coefficients is expected to vary only slightly with ϵ_C and has been calculated [56] to be about 0.85 at $\epsilon = 0$ to about 0.87 at $\epsilon = 0.2$. The ratio R^2_{gC}/R^2_{gR} for Gaussian chains and $\epsilon_C = 0$ has been calculated [50] to be 2, its dependence on chain stiffness in the Kratky–Porod wormlike model can be derived from the Fujii–Yamakawa treatment [59].

We can now apply the considerations developed above to the DNA we have studied in this work. Fortunately the choice of both the DNA itself and the experimental conditions allow interpretation at the present state of the art of both theory and experiment. For the size of the DNA used, laser light scattering to minimum values of $\theta = 7°$ is adequate for extrapolation to forward angles and does not give rise to ambiguities previously encountered in DNA light scattering work (cf. refs. [13,14,43]). Non-Newtonian effects in viscosity are absent in the Zimm-Crothers viscometer used and, as was demonstrated above, even in the convenient variable level, capillary viscometer. Velocity and pressure effects in sedimentation are definitely not encountered and straightforward boundary sedimentation can be used under a variety of conditions. At this molecular weight (4.3×10^6) excluded volume effects may be ignored; we have reason to believe [18] that even for higher molecular weight DNA (up to 10^8) excluded volume effects have been largely overestimated. Polyelectrolyte effects on conformation are of very little consequence at an ionic strength of about 0.2 M NaCl (the characteristic Debye radius $1/\kappa$ which determines the range of electrostatic interactions is about 1.4 nm at this ionic strength; electrostatic interactions are therefore not likely to influence largely [45] the size of a statistical Kuhn element of DNA of about 110 nm. At considerably lower salt concentrations, electrostatic effects could assume increase significance, yet at the presently used and higher ionic strengths, they can be disregarded. The DNA is large enough (about $L' = L/2a = 22$ Kuhn statistical elements in a contour length L of 2210 nm) to approach coil-like behavior and disregard complications arising for almost fully stretched rods. We therefore may disregard excluded volume in our analysis and assume a value of ϵ equal to 0.2, the origin of which is mostly attributed to the non-Gaussian character of the coils deriving from chain stiffness (fig. 2 of ref. [62]).

In the sedimentation experiment it is possible to distinguish between a weight-average sedimentation coefficient $\langle s_{20,w}\rangle_w$ and $s_{20,w}$ for the individual species. Thus, whereas $(s^0_{20,w})_C/s^0_{20,w})_R$ equals 0.87 (column c of table 2), in good agreement with theoretical predictions (fig. 2 of ref. [56]; from ref. [59] we calculate 0.88 for wormlike rings without excluded volume), the value of the ratio experimentally obtained for the weighted average (form II contains contamination from both forms I and III, see above) is only 0.81 (column d of table 2).

In the viscosity results we must perforce consider the experimentally obtained weighted average (column h of table 2) and find 1.83 for $[\eta]_C/[\eta]_R$. This is close to the theoretical prediction of about 1.7 (fig. 1 of ref. [56]) or 1.8 calculated from ref. [59] (we have not attempted to take cross contamination of the various species into consideration).

The diffusion coefficients from light scattering can in principle be obtained for the pure circular form II in the presence of the other forms (the linear form III has been obtained in a pure state) yet in practice this has not been achieved. We derive the z-average of D and find that the ratio $(\langle D^0_{20,w}\rangle_{zC}/(\langle D^0_{20,w}\rangle_z)_R$ equals 0.81 (column e of table 2), the same as for the ratio of

the weighted sedimentation coefficients, which is just another statement that the Svedberg eq. (6) yields the same weight-average molecular weights for both forms (column f of table 2; identical values of ϕ' are taken).

The experimental value for $s_{20,w} = 16.3$ for the linear coil form III falls precisely on the calculated curve (fig. 8 of ref. [18]) of Godfrey and Eisenberg, whereas the corresponding value of $[\eta] = 26.05$ dl/g falls slightly below the calculated curve (fig. 10 of ref. [18]). Without intent to unduly stress this point we recall that (in distinction to the sedimentation calculation) the calculated viscosity curve gave an unreasonably low chain diameter; the present result can be well fitted on an empirical plot with the previous data (fig. 10 of ref. [18]). The values of the second virial coefficients A_2, the Huggins coefficient k, and the Flory–Mandelkern parameter β in table 2 are in agreement with expected values for these parameters.

Next we analyze the light scattering results. From $R_g = 186$ nm of the linear form III we calculate by the exact equation of Benoit and Doty [65]

$$\frac{R_g^2}{4a^2} = \frac{L'}{6} - \frac{1}{4} + \frac{1}{4L'} - \frac{1 - e^{-2L'}}{8L'^2} \qquad (11)$$

a persistence length $a = 50$ nm. This is slightly lower than the value $a = 54$ nm determined by Godfrey and Eisenberg [18] for a series of well characterized fractions of calf-thymus DNA ($0.3 < M_w\ 10^{-6} < 1.3$). It is significantly lower though than the value $a = 66$ nm reported by Jolly and Eisenberg [17] for a fraction of calf-thymus DNA with $M_w = 3.75 \times 10^6$. These authors report $R_g = 206.9$ nm which was obtained from the slope of the limiting Zimm plot. If, in line with considerations presented above with respect to the true initial slope for values of X larger than 0.3, we reduce this value of R_g by about 10%, then the persistence length is reduced by about 20% (for linear coils $R_g^2 \sim La$) and becomes close to the value reported here for a monodisperse plasmid DNA sample. The values for a of Godfrey and Eisenberg [18] were obtained from lower molecular weight samples, albeit at somewhat higher values of the scattering angle ($\theta \geqslant 17^0$) and should probably also be reduced to some extent. The value of about 50 nm for the persistence length of the wormlike chain model, calculated from light scattering on the basis of exact expressions appears to be somewhat lower than that (about 60 nm) derived from viscosity and sedimentation data on the basis of complicated hydrodynamic theory. The hydrodynamic behavior also weakly depends on a hydrodynamic diameter of the DNA coils, a parameter not appearing in the interpretation of the scattering results.

We note (ref. [60], fig. 1 as well as ref. [66], fig. 1) that for values $L' = 22$ (this work), the scattering curve for form III should coincide with that of a Gaussian coil for values $X < 10$. It is not surprising therefore that all our measurements (fig. 10, top set of data) for form III for $X < 7$ fall on the random coil curve. We would expect a similar behavior for the circular form II (fig. 10, middle set of data) where our measurements only extend to $X < 4$. For the value $L' = 22$ applicable to our DNA the theoretical ratio $R_{gC}^2/R_{gR}^2 = 1.97$ calculated by Fujii and Yamakawa [59] is also close to the random coil value 2 calculated by Casassa [50]; we find (column 6, table 2) 1.92 from our experimental results.

Dawson and Harpst [67] find $R_{gC}^2/R_{gR}^2 = 1.22$, for the much higher molecular weight (33×10^6) λ-DNA. We would expect this DNA, which has a chain length one order of magnitude higher than our DNA, to approach the Gaussian coil behavior even more closely and excluded volume effects should not yet be appreciable; on the experimental level it may be that a lower limit scattering angle used by the authors [67] was not low enough for the analysis used.

Finally with R_g of form III precisely known from the scattering at low angles (top curve, fig. 10) it is possible now to scale our results at high angles of scattering (θ up to 150°) for comparison (fig. 13) with the scattering functions [60,66] for stiff coils without excluded volume, for various values of the reduced contour length L', the number of Kuhn statistical elements in the chain; L' infinity corresponds to the gaussian coil, $L' = 0$ is the rigid rod and for the intermediate values of L' eq. (B-3) of Sharp and Bloomfield [66] has been used (a factor 15 is missing in the denominator of the last term. The more elaborate calculation of Yamakawa and Fujii [60] yields very similar results for value $L' \geqslant 10$, and $q^2 \leqslant 10$). $P^{-1}(\theta)$ is uniquely determined by X and L' and it was a great source of satisfaction to find the experimental results closely following the scattering curve for $L' = 21$, at values X as high as 35. We recall that the value expected from the limiting values of X (independent of a specific model for the DNA coil) was 22 and the agreement is excellent in view of the close spacing of

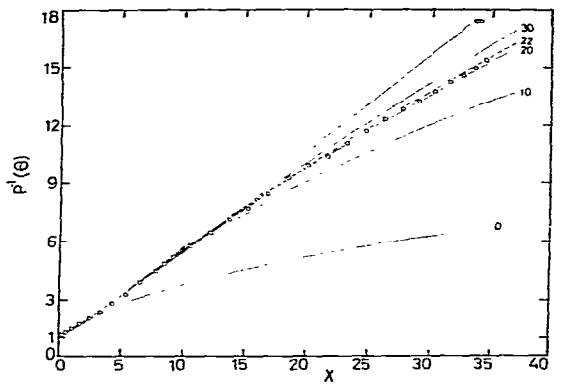

Fig. 3. Angular dependence of scattering of ColE$_1$-plasmid DNA, Form III, at high scattering angles. Experimental points from fig. 8, normalized to unity at $X = 0$ (from the data of low angles) and scaled to $X \equiv q^2 R_g^2 (R_g = 186$ nm). Theoretical curves for $L' \equiv L/2a = \infty$ (gaussian coils), $L' = 30$, 22, 20, 10 (stiff coils, refs. [60,66]) and $L' = 0$ (rigid rods).

the theoretical scattering curves. Under less fortunate circumstances the experimental data might have cut across a family of theoretical curves.

5. Conclusions

In conclusion we may state that it is now possible to examine a surprisingly homogeneous DNA system under various experimental conditions. The physical methods used correctly characterize the system within very reasonable limits. There therefore seems to be no doubt that true physical constants can be established and conformational changes can be studied in various solvent and ligand systems and in combination with suitably chosen proteins, thus establishing a relationship to situations of biological interest.

At the present state of the art, both the DNA systems as well as the experimental data can be faithfully reproduced and a precise absolute molecular weight scale could be established for this and other plasmid DNA's relative to a suitable reference, such as SV-40 DNA, for instance. Hydrodynamic and scattering theories can be critically verified to a previously unattainable level of reliability and precision.

Acknowledgements

This study was supported by a grant from the Israel-US Binational Foundation, Jerusalem, Israel.

The authors are indebted to Dorit Kalif and Yeheskiel Haik for expert technical assistance and to Drs. V. Benghiat, M.A. Hirshfeld, S. Sarid, T. Vogel and G. Zaichek (of the Hebrew University) for practical advice on help and stimulating discussion. We thank Prof. H. Yamakawa for supplying extensive tables for numerical values based on ref. [59].

One of us (G.V.) acknowledges the generous support of a National Research Council of Canada Postdoctoral Fellowship. Z.K. is the incumbent of the Pollack Career Development Chair at the Weizmann Institute of Science. G.V. is now in the Biochemistry Department, The Agricultural University, Wageningen.

References

[1] D.R. Hewish and L.A. Burgoyne, Biochem. Biophys. Res. Commun. 52 (1973) 504.
[2] K.E. Van Holde and I. Isenberg, Acc. Chem. Res. 8 (1975) 327.
[3] R.D. Kornberg, Science 184 (1974) 868.
[4] A.L. Olins and D.E. Olins, Science 183 (1974) 330.
[5] P. Oudet, M. Gross-Bellard and P. Chambon, Cell 4 (1975) 281.
[6] J.E. Germond, B. Hirth, P. Oudet, M. Gross-Bellard and P. Chambon, Proc. Nat. Acad. Sci. USA 72 (1975) 1843.
[7] G. Voordouw, D. Kalif and H. Eisenberg, Nucl. Ac. Res. 4 (1977) 1207.
[8] G. Voordouw and H. Eisenberg, Nature, in press.
[9] G. Voordouw, Z. Kam, N. Borochov and H. Eisenberg, in preparation.
[10] J.D. Watson and F.H.C. Crick, Nature 171 (1953) 737.
[11] W. Bauer and J. Vinograd, in: Basic principles in nucleic acids, Vol. 2, ed. P.O.P. Ts'o (Academic Press, New York, 1974) Chapter 4.
[12] A. Kornberg, DNA synthesis (W.H. Freeman and Company, San Francisco, 1974).
[13] H. Eisenberg, in: Basic principles in nucleic acids, Vol. 2, ed. P.O.P. Ts'o (Academic Press, New York, 1974) Chapter 3.
[14] V.A. Bloomfield, D.M. Crothers and I. Tinoco, Physical chemistry of nucleic acids (Harper and Row, New York, 1974) Chapter 5.
[15] G. Cohen and H. Eisenberg, Biopolymers 4 (1966) 429.
[16] J.E. Godfrey, Biophys. Chem. 5 (1976) 285.
[17] D. Jolly and H. Eisenberg, Biopolymers 15 (1976) 61.
[18] J.E. Godfrey and H. Eisenberg, Biophys. Chem. 5 (1976) 301.

[19] O. Kratky and G. Porod, Rec. Trav. Chim. 68 (1949) 1106.
[20] P.J. Flory, Statistical mechanics of chain molecules (Interscience Publishers, New York, 1969) Appendix G.
[21] D.B. Clewell, J. Bact. 110 (1972) 667.
[22] D.B. Clewell and D.R. Helinski, Proc. Nat. Acad. Sci. USA 62 (1969) 1159.
[23] D.B. Clewell and D.R. Helinski, Biochemistry 9 (1970) 4428.
[24] D.G. Blair and D.R. Helinski, J. Biol. Chem. 250 (1975) 8785.
[25] M.A. Lovett and D.R. Helinski, J. Biol. Chem. 250 (1975) 8790.
[26] D.G. Guiney and D.R. Helinski, J. Biol. Chem. 250 (1975) 8796.
[27] M.A. Lovett, L. Katz and D.R. Helinski, Nature 251 (1974) 337.
[28] C.W. Schmid, F.P. Rinehart and J.E. Hearst, Biopolymers 10 (1971) 883.
[29] C.W. Schmid and J.E. Hearst, J. Mol. Biol. 44 (1969) 143.
[30] D.J. Jolly and A.M. Campbell, Biochem. J. 128 (1972) 569; 1019.
[31] A.M. Campbell and J.D. Jolly, Biochem. J. 133 (1973) 209.
[32] R.C. Clowes and W. Haynes, Experiments in microbial genetics (John Wiley and Sons, Inc., New York, 1968) p. 187.
[33] P. Guerry, D.J. Le Blanc and S. Falkow, J. Bact. 116 (1973) 1064.
[34] R. Radloff, W. Bauer and J. Vinograd, Proc. Nat. Acad. Sci. USA 57 (1967) 1514.
[35] W.R. Morrison, Anal. Biochem. 7 (1964) 218.
[36] V.N. Schumaker and H.K. Schachman, Biochim. Biophys. Acta 23 (1957) 628.
[37] H. Eisenberg, Biological macromolecules and polyelectrolytes in solution (Clarendon Press, Oxford, 1976).
[38] E. Jakeman, G.J. Oliver, E.R. Pike and P.N. Pusey, Proc. Phys. Soc. Lond. 5 (1972) L93.
[39] D.E. Koppel, J. Chem. Phys. 57 (1972) 4814.
[40] J.P. Kratohvill, G. Dezelic, M. Kerker and E. Matijevic J. Polym. Sci. 57 (1962) 59.
[41] G. Cohen and H. Eisenberg, J. Phys. Chem. 43 (1965) 3881.
[42] B.H. Zimm, J. Chem. Phys. 16 (1948) 1099.
[43] H. Eisenberg, in: Procedures in nucleic acids, Vol. 2, eds. G.L. Cantoni and D.R. Davies (Harper and Row, New York, 1976) p. 137.
[44] B.H. Zimm and D.M. Crothers, Proc. Nat. Acad. Sci. USA 48 (1962) 905.
[45] H. Eisenberg, J. Polym. Sci. 25 (1957) 257.
[46] S.H. Maron and R.J. Belner, J. Appl. Phys. 26 (1965) 1457.
[47] A.V. Kleinschmidt, Methods Enzymol. 12B (1968) 361.
[48] S.Z. Hirschmann and G. Felsenfeld, J. Mol. Biol. 16 (1966) 347.
[49] J. Inselburg and M. Fuke, Proc. Nat. Acad. Sci. USA 68 (1971) 2839
[50] E.F. Casassa, J. Polymer Sci. A 3 (1965) 605.
[51] H.A. Kramers, J. Chem. Phys. 14 (1946) 415.
[52] B.H. Zimm and W.H. Stockmayer, J. Chem. Phys. 17 (1949) 1301.
[53] W. Fiers and R.L. Sinsheimer, J. Mol. Biol. 5 (1962) 424.
[54] R. Weil and J. Vinograd, Proc. Nat. Acad. Sci. USA 50 (1963) 730.
[55] M. Böttger, D. Bierwolf, V. Wunderlich and A. Graffi, Biochim. Biophys. Acta 232 (1971) 21.
[56] V. Bloomfield and B.H. Zimm, J. Chem. Phys. 44 (1966) 315.
[57] M. Fukatsu and M. Kurata, J. Chem. Phys. 44 (1966) 4539.
[58] H.B. Gray Jr., V.A. Bloomfield and J.E. Hearst, J. Chem. Phys. 46 (1967) 1493.
[59] M. Fujii and H. Yamakawa, Macromolecules 8 (1975) 792.
[60] H. Yamakawa and M. Fujii, Macromolecules 7 (1974) 649.
[61] R.J. Douthart and V.A. Bloomfield, Biopolymers 6 (1968) 1297.
[62] A. Opschoor, P.H. Pouwels, C.M. Knijnenburg and J.B.T. Aten, J. Mol. Biol. 37 (1968) 13.
[63] J.C. Wang, J. Mol. Biol. 43 (1969) 263.
[64] W.B. Upholt, H.B. Gray, Jr. and J. Vinograd, J. Mol. Biol. 61 (1971) 21.
[65] H. Benoit and P. Doty, J. Phys. Chem. 57 (1953) 958.
[66] P. Sharp and V.A. Bloomfield, Biopolymers 6 (1968) 1201.
[67] J.R. Dawson and J.A. Harpst, Biopolymers 10 (1971) 2499.